Published in final edited form as:
Science. 2012 June 1; 336(6085): 1168–1171. doi:10.1126/science.1219988.

The Amyloid Precursor Protein has a Flexible Transmembrane Domain and Binds Cholesterol

Paul J. Barrett[1,*], **Yuanli Song**[1,*], **Wade D. Van Horn**[1], **Eric J. Hustedt**[2], **Johanna M. Schafer**[1], **Arina Hadziselimovic**[1], **Andrew J. Beel**[1], and **Charles R. Sanders**[1,†]

[1]Dept. of Biochemistry, Center for Structural Biology and Institute of Chemical Biology, Vanderbilt University School of Medicine, Nashville, TN 37232, USA

[2]Dept. of Molecular Physiology and Biophysics, Vanderbilt University School of Medicine, Nashville, TN 37232, USA

Abstract

C99 is the transmembrane carboxyl-terminal domain of the amyloid precursor protein that is cleaved by γ-secretase to release the amyloid-β polypeptides, which are associated with Alzheimer's disease. Nuclear magnetic resonance and electron paramagnetic resonance spectroscopy show that the extracellular amino terminus of C99 includes a surface-embedded "N-helix" followed by a short "N-loop" connecting to the transmembrane domain (TMD). The TMD is a flexibly curved α helix, making it well suited for processive cleavage by γ-secretase. Titration of C99 reveals a binding site for cholesterol, providing mechanistic insight into how cholesterol promotes amyloidogenesis. Membrane-buried GXXXG motifs (G, Gly; X, any amino acid), which have an established role in oligomerization, were also shown to play a key role in cholesterol binding. The structure and cholesterol binding properties of C99 may aid in the design of Alzheimer's therapeutics.

Alzheimer's disease (AD) currently afflicts more than 20 million people worldwide (1). The production and subsequent aggregation of amyloid-β (Aβ) peptides are widely thought to play a central role in most forms of AD (1, 2); accordingly, factors that increase Aβ production and oligomerization or that reduce its elimination increase the risk of AD. Elevated neuronal cholesterol levels increase the generation of Aβ (3–5), but the underlying mechanisms have yet to be elucidated.

Amyloidogenic cleavage of full-length amyloid precursor protein (APP) by β-secretase generates the transmembrane protein C99 ($APP_{672–770}$, also known as β-CTF, fig. S1). The transmembrane domain (TMD) of C99 is then processively but imprecisely cleaved by γ-secretase to release the Aβ polypeptides (6, 7). Structural information on C99 may provide insight into amyloidogenesis; however, previous structural studies have employed only low-resolution methods or have focused on TMD-containing fragments (8–12).

The backbone structure of C99 in lyso-myristoylphosphatidylglycerol (LMPG) detergent micelles was determined by nuclear magnetic resonance (NMR) restraints that included

†To whom correspondence should be addressed. chuck.sanders@vanderbilt.edu.
*These authors contributed equally to this work.

Supplementary Materials
Materials and Methods
Figs. S1 to S9
Table S1
References (34–44)

residual dipolar couplings and distances derived from paramagnetic relaxation enhancement experiments (Fig. 1, figs. S2 and S3, and table S1). To prevent dimerization (11–14), we used an 800:1 LMPG-to-C99 molar ratio (see supplemental materials and methods). C99 is composed of three helical domains. A short extracellular "N-helix"(residues 688 to 694) is connected by an interfacial "N-loop" (695 to 699) to the helical TMD (700 to 723). The N-helix is embedded in the membrane surface and dynamically samples a range of orientations around the TMD helix axis (Fig. 1B). A third helix at the C terminus (residues 762 to 770) is surface-associated but is structurally uncoupled from the TMD by the intervening 38-residue "C-loop" (734 to 761). Power saturation electron paramagnetic resonance (EPR) measurements for spin-labeled C99 (Fig. 2 and fig. S4) confirm that the span of the TMD is the same in both micelles and lipid vesicles and that the N- and C-helices are surface-associated.

The NMR structure reveals that the TM helix of C99 is highly curved, with the apex of curvature being located near glycine residues 708 and 709, close to the center of the micelle (Fig. 1). Pulsed EPR double electron-electron resonance (DEER) experiments confirmed that the TMD curvature also occurs in lipid bilayers (Fig. 2 and fig. S5). The measured end-to-end average distance in micelles (34.2 ± 1.1 Å) is consistent with the NMR structure and nearly identical to the distance measured in lipid vesicles (33.5 ± 1.0 Å). With the use of EPR, we found that mutation of $G_{708}G_{709}$ to $L_{708}L_{709}$ (G, Gly; L, Leu) only modestly straightens the helix (average distance now 35.3 ± 0.5 Å), suggesting that the curvature of the TMD derives only partially from the glycine pair (Fig. 2C). However, the ranges of distances sampled around the mean by the $Gly^{708}\rightarrow Leu^{708}$ (G708L) and G708L/G709L mutants are dramatically reduced compared with those of the wild type (Fig. 2C). This suggests that Gly_{708} confers flexibility to the TMD, as predicted by molecular dynamics simulations (15). The flexibly curved nature of the TMD may be well suited for its interactions with γ-secretase. Medium-resolution electron microscopy structures of the fully assembled and activated γ-secretase (16, 17) suggest a sluice-like active site that might best accommodate a substrate with a curved TMD (see docking model in fig. S6). Analogous active sites have been observed for other intramembrane proteases (18, 19). TMD flexibility may also promote the processive cleavage of C99 by γ-secretase, with flexibility colluding with random thermal motion to allow the TMD to slide through the active-site channel. Curvature may also play a role in exposing scissile bonds for proteolytic access. The surface-associated N-helix and N-loop immediately following the cleavage site (K687; K, Lys) for nonamyloidogenic α-secretase processing contain a number of familial AD mutation sites (20) and, in conjunction with the extracellular end of the TMD, appear to play crucial roles in determining the ratio of short versus the more toxic long forms of the Aβ peptides released by γ-secretase (13, 14). A space-filling surface representation (Fig. 1C) of C99 suggests that these segments may also partially occlude approach by another TMD to the glycine zipper GXXXGXXXG (X, any amino acid) sequence located on the extracellular end of the TMD, which helps to explain the weakness of C99 self-association.

The organization of the N-loop and N-helix with respect to the membrane surface and the TMD is consistent with the possibility of a lipid binding site centered around the N-helix/N-loop/TMD structural element, as suggested by previous studies (10, 11). Titrations of C99 with cholesterol were carried out using bicelles as the model membranes because this medium is able to solubilize cholesterol up to ~20 mole percent (mol %). Cholesterol titration of C99 results in substantial changes in NMR resonance positions for a subset of C99 peaks (Fig. 3A). The shifts in these peaks saturate at high cholesterol concentrations and can be fit by a 1:1 binding model, indicating a dissociation constant (K_d) of 5.1 ± 1.2 mol % (Fig. 3B), which falls within the range of cholesterol concentrations in mammalian plasma and organelle membranes (21), supporting the physiological relevance of this complex.

Full-length APP is likely to bind cholesterol with an avidity similar to C99 because its ectodomain is expected to have no influence on the architecture of the cholesterol binding site.

The resonances in C99 exhibiting the most profound shifts in response to cholesterol are all localized to the N-helix, N-loop, and extracellular end of the TMD and include G700, G704, and G708 (Fig. 3C). To identify specific residues critical to cholesterol binding, we employed alanine scanning mutagenesis to replace each residue in the 690 to 710 range, followed by cholesterol titrations (Fig. 3, D and E, and figs. S7 and S8). Mutations at some sites eliminated detectable cholesterol binding, even at 20 mol % cholesterol (Fig. 3E). The cholesterol binding site of C99 involves residues from the N-helix, N-loop, and TMD and is different from previously characterized cholesterol binding sites in proteins (22). Based on Fig. 3C, it is likely that N698 (N, Asn) donates a hydrogen bond to the hydroxyl head group of cholesterol, whereas E693 (E, Glu) accepts a hydrogen bond. Also essential to cholesterol binding are G700 and G704, located in the tandem GXXXG motifs of the TMD and, to a lesser degree, G708. GXXXG motifs and the related GXXXGXXXG glycine zipper sequence have long been recognized as common structural elements that can drive homo- or hetero-oligomerization of membrane proteins (23–25). Though there has been much interest in the possibility that these motifs drive homodimerization of C99 (12–15, 25), our observation that the GXXXG motifs are critical for cholesterol binding indicates an additional role for these motifs in C99. It should be added that the $G_{700}AIIG_{704}$ segment has been shown to be important in establishing the production ratio between long and short forms of the Aβ polypeptides by γ-secretase (13, 14) and in making that ratio susceptible to alterations by druglike small molecules known as γ-secretase modulators (26, 27).

A space-filling surface representation shows that G700 and G704 are located on the outer face of the curved TM helix and result in that face of the helix having a locally flat surface (Fig. 1C), which is probably optimal for van der Waals interactions with cholesterol, which itself is relatively flat. Pairing the surface afforded by the GXXXG motifs with a rigid cholesterol molecule is expected to be entropically advantageous compared with association with more flexible lipids.

Binding of cholesterol to C99 appears to rely on the flexibility of the N-loop to allow induced-fit conformational changes required to optimize interactions of cholesterol with key residues in this loop and in the N-helix (fig. S9). This is supported by observation of a number of N-loop residues for which substantial changes in NMR resonance chemical shifts are observed in response to cholesterol binding [e.g., S697 (S, Ser), see Fig. 3D] but that do not appear to make direct contacts with the lipid (Fig. 3E).

The literature suggests plausible mechanisms by which complex formation between C99 or APP and cholesterol contributes to amyloidogenesis and AD. First, there are numerous reports that β- and γ-secretase associate with cholesterol-rich membrane domains often referred to as “lipid rafts” (4, 5, 28, 29). Association of C99/APP with cholesterol may favor partitioning of the protein into membrane domains enriched in the proteases of the amyloidogenic pathway. Second, cholesterol binding to C99 may play a cofactor role to promote substrate recognition or catalysis. The addition of cholesterol to purified γ-secretase in model membranes enhances the cleavage rate of purified C99 in lipid vesicles (30). Third, given that the α-secretase cleavage site (K687) is immediately adjacent to the cholesterol binding site, direct binding of cholesterol to APP could reduce nonamyloidogenic cleavage by α-secretase (31, 32). Finally, the cholesterol binding site in C99 is contained within its amyloid-β domain (C99 residues 672 to 711 correspond to $Aβ_{40}$), such that complex formation between cholesterol and Aβ may contribute to the known profibrillogenic effect of membrane cholesterol (33).

In conclusion, determination of the structure of C99 and the observation that it forms an avid complex with cholesterol provide insight into amyloidogenesis. The flexibly curved TMD of C99 offers insight into how it is recognized and proteolyzed by γ-secretase, and the discovery that its GXXXG segments play critical roles in cholesterol binding reveals a previously unrecognized function for these motifs. The structure of C99 can potentially assist the design and optimization of C99-selective AD therapeutics that act by altering its interactions with γ-secretase. Moreover, development of compounds that prevent binding of cholesterol to C99 or APP may have prophylactic utility in AD.

Supplementary Material

Refer to Web version on PubMed Central for supplementary material.

Acknowledgments

This work was supported by Alzheimer's Association grant IIRG-07-59379, NIH grants PO1 GM080513 (C.R.S. and E.J.H.) and T32 GM08320(P.J.B.), and by an American Heart Association grant AHA10POST4210008 (W.D.V.H.). We thank S. Howell for technical assistance and F. Sönnichsen, K. Mittendorf, B. Carter, E. Stanley, and C. Deatherage for comments on this manuscript. Coordinates for the structure of C99 have been deposited in the Protein Data Bank (accession code 2LP1).

References and Notes

1. O'Brien RJ, Wong PC. Annu. Rev. Neurosci. 2011; 34:185. [PubMed: 21456963]
2. Haass C, Selkoe DJ. Nat. Rev. Mol. Cell Biol. 2007; 8:101. [PubMed: 17245412]
3. Fonseca AC, Resende R, Oliveira CR, Pereira CM. Exp. Neurol. 2010; 223:282. [PubMed: 19782682]
4. Simons M, et al. Proc. Natl. Acad. Sci. U.S.A. 1998; 95:6460. [PubMed: 9600988]
5. Wahrle S, et al. Neurobiol. Dis. 2002; 9:11. [PubMed: 11848681]
6. Kukar TL, et al. J. Biol. Chem. 2011; 286:39804. [PubMed: 21868378]
7. Takami M, et al. J. Neurosci. 2009; 29:13042. [PubMed: 19828817]
8. Lu JX, Yau WM, Tycko R. Biophys. J. 2011; 100:711. [PubMed: 21281586]
9. Botev A, et al. Biochemistry. 2011; 50:828. [PubMed: 21186781]
10. Nadezhdin KD, Bocharova OV, Bocharov EV, Arseniev AS. Acta Naturae. 2011; 2010:69. [PubMed: 22649674]
11. Beel AJ, et al. Biochemistry. 2008; 47:9428. [PubMed: 18702528]
12. Sato T, et al. Proc. Natl. Acad. Sci. U.S.A. 2009; 106:1421. [PubMed: 19164538]
13. Kienlen-Campard P, et al. J. Biol. Chem. 2008; 283:7733. [PubMed: 18201969]
14. Munter LM, et al. EMBO J. 2007; 26:1702. [PubMed: 17332749]
15. Miyashita N, Straub JE, Thirumalai D. J. Am. Chem. Soc. 2009; 131:17843. [PubMed: 19995075]
16. Osenkowski P, et al. J. Mol. Biol. 2009; 385:642. [PubMed: 19013469]
17. Renzi F, et al. J. Biol. Chem. 2011; 286:21440. [PubMed: 21454611]
18. Urban S. Biochem. J. 2010; 425:501. [PubMed: 20070259]
19. Wolfe MS. Chem. Rev. 2009; 109:1599. [PubMed: 19226105]
20. Hardy J, Crook R. Alzheimer Research Forum. 2012 www.alzforum.org/res/com/mut/app/.
21. van Meer G, Voelker DR, Feigenson GW. Nat. Rev.Mol. Cell Biol. 2008; 9:112. [PubMed: 18216768]
22. Epand RM. Biochim. Biophys. Acta. 2008; 1778:1576. [PubMed: 18423371]
23. Lemmon MA, et al. J. Biol. Chem. 1992; 267:7683. [PubMed: 1560003]
24. MacKenzie KR, Prestegard JH, Engelman DM. Science. 1997; 276:131. [PubMed: 9082985]
25. Kim S, et al. Proc. Natl. Acad. Sci. U.S.A. 2005; 102:14278. [PubMed: 16179394]
26. Kukar TL, et al. Nature. 2008; 453:925. [PubMed: 18548070]

27. Sagi SA, et al. J. Biol. Chem. 2011; 286:39794. [PubMed: 21868380]
28. Ehehalt R, Keller P, Haass C, Thiele C, Simons K. J. Cell Biol. 2003; 160:113. [PubMed: 12515826]
29. Lee SJ, et al. Nat. Med. 1998; 4:730. [PubMed: 9623986]
30. Osenkowski P, Ye W, Wang R, Wolfe MS, Selkoe DJ. J. Biol. Chem. 2008; 283:22529. [PubMed: 18539594]
31. Bodovitz S, Klein WL. J. Biol. Chem. 1996; 271:4436. [PubMed: 8626795]
32. Kojro E, Gimpl G, Lammich S, Marz W, Fahrenholz F. Proc. Natl. Acad. Sci. U.S.A. 2001; 98:5815. [PubMed: 11309494]
33. Yanagisawa K. Subcell. Biochem. 2005; 38:179. [PubMed: 15709479]
34. Eisele YS, et al. Mol. Biol. Cell. 2007; 18:3591. [PubMed: 17626163]
35. Shen Y, Delaglio F, Cornilescu G, Bax A. J. Biomol. NMR. 2009; 44:213. [PubMed: 19548092]
36. Wishart DS, Sykes BD. Methods Enzymol. 1994; 239:363. [PubMed: 7830591]
37. Johnson BA. Methods Mol. Biol. 2004; 278:313. [PubMed: 15318002]
38. Chen K, Tjandra N. J. Biomol. NMR. 2007; 38:303. [PubMed: 17593526]
39. Delaglio F, et al. J. Biomol. NMR. 1995; 6:277. [PubMed: 8520220]
40. Battiste JL, Wagner G. Biochemistry. 2000; 39:5355. [PubMed: 10820006]
41. Shen Y, Delaglio F, Cornilescu G, Bax A. J. Biomol. NMR. 2009; 44:213. [PubMed: 19548092]
42. Schwieters CD, Kuszewski JJ, Tjandra N, Clore GM. J. Magn Reson. 2003; 160:65. [PubMed: 12565051]
43. Altenbach C, Greenhalgh DA, Khorana HG, Hubbell WL. Proc. Natl. Acad. Sci. U.S. A. 1994; 91:1667. [PubMed: 8127863]
44. Jeschke G. Annu. Rev. Phys. Chem. 2012; 63:419. [PubMed: 22404592]

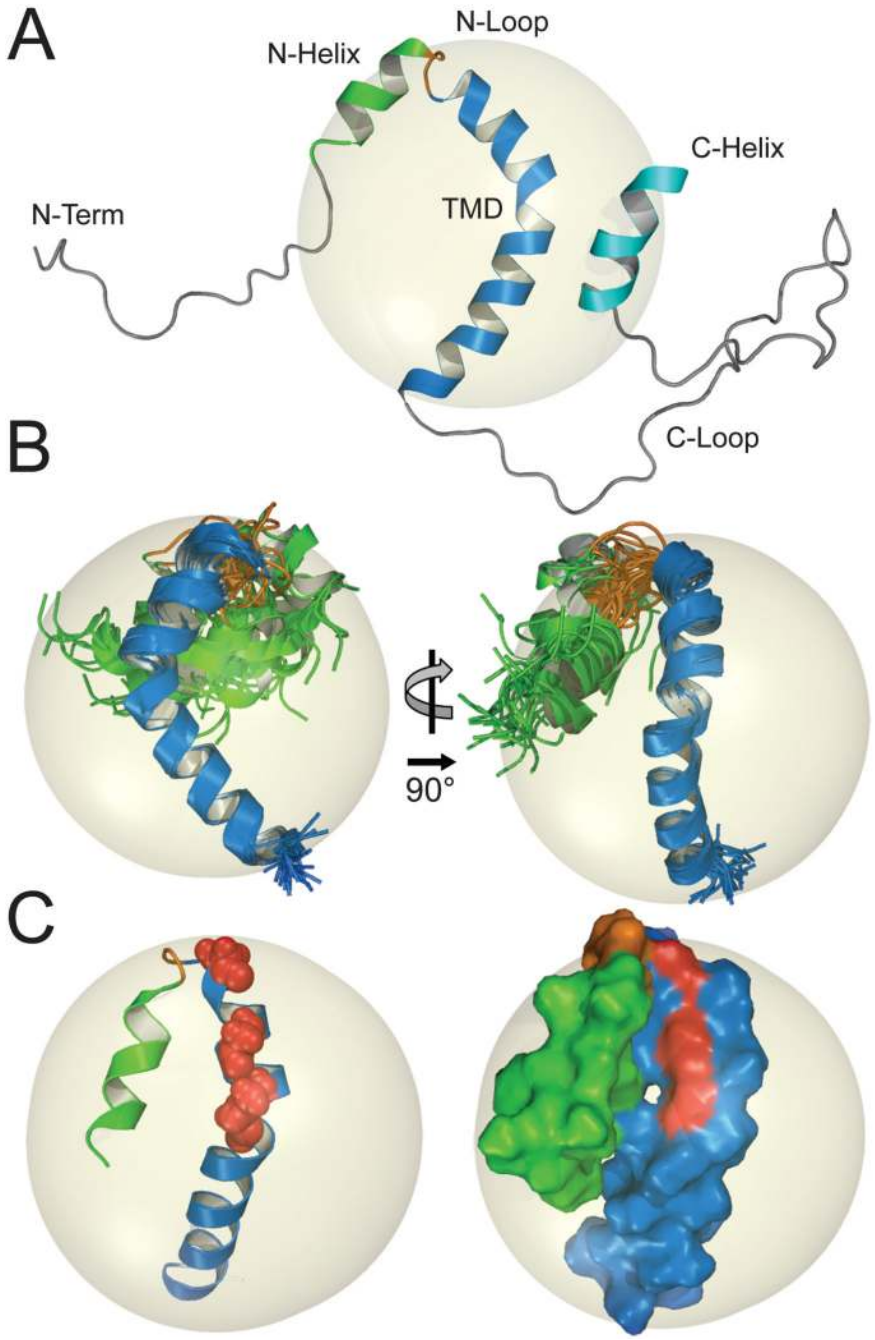

Fig. 1.

Structure of C99 in lyso-myristoylphosphatidylcholine (LMPG) micelles. (**A**) Representative structure from a preliminary structural ensemble that illustrates the disorder of the N terminus and C loop and the interfacial location of the C helix. The 35 Å sphere inscribed on the structures of this figure represents a detergent micelle. (**B**) The 30 lowest-energy structures in which the disordered N terminus (residues 672 to 685) and cytosolic domain (726 to 770) are omitted. (**C**) Representative structure from (B) with atoms for glycine residues 700, 704, 708, and 709 highlighted in van der Waals mode.

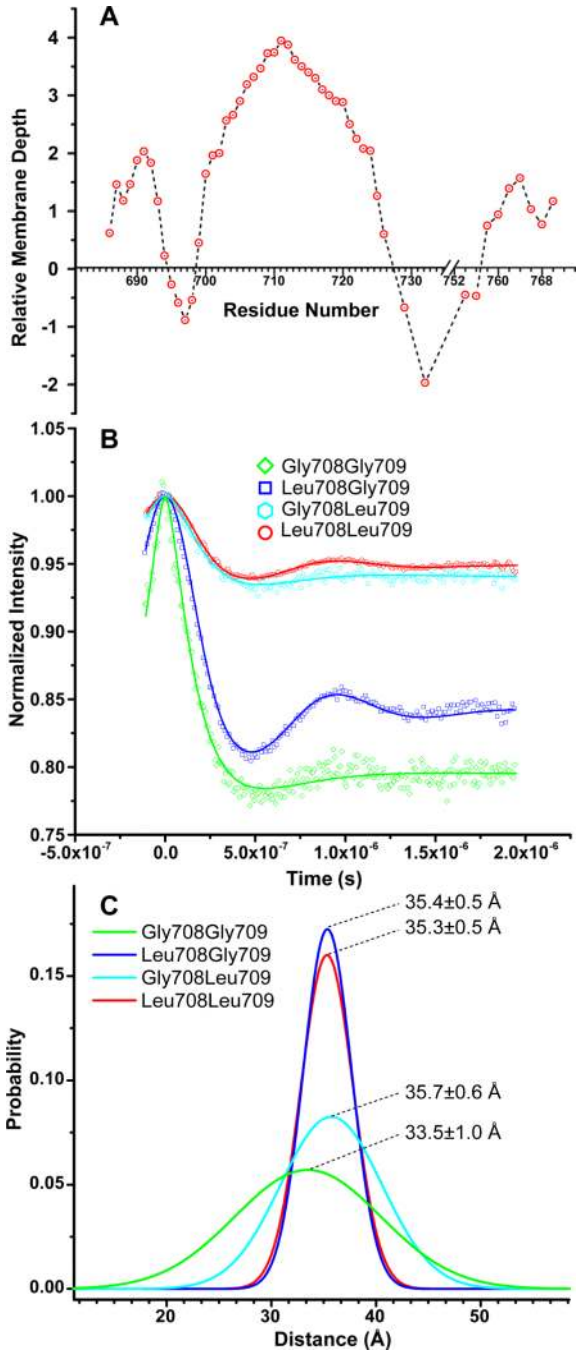

Fig. 2.

EPR studies of C99 in 1:4 1-palmitoyl-2-oleoyl-phosphatidylglycerol:1-palmitoyl-2-oleoyl-phosphatidylcholine lipid vesicles. (**A**) Bilayer depth parameters measured for spin-labeled sites on C99 as determined from power saturation EPR measurements. Positive values indicate burial in the membrane, whereas negative values indicate exposure to water. Though the samples used for NMR structural determination contained a C-terminal purification tag (see caption to fig. S1), the samples used for measurements involving the C-terminal sites (752 to 770) did not contain this tag, such that these measurements verify that the membrane association of the C terminus is not the result of the presence of a non-native tag sequence. (**B**) X-band DEER time evolutions measured at 80 K for C99 that was spin-

labeled at the ends of its TMD (at sites 700 and 723). Results are shown for C99 with its wild-type (WT) sequence, except for the two spin-labeled sites, and for C99 that was additionally subjected to Gly-to-Leu mutations at G708 and G709. (**C**) Distance distributions between the spin labels measured from the DEER data from (B). The SD associated with each average distance relates to the uncertainty of the average, not to the population distribution around the average.

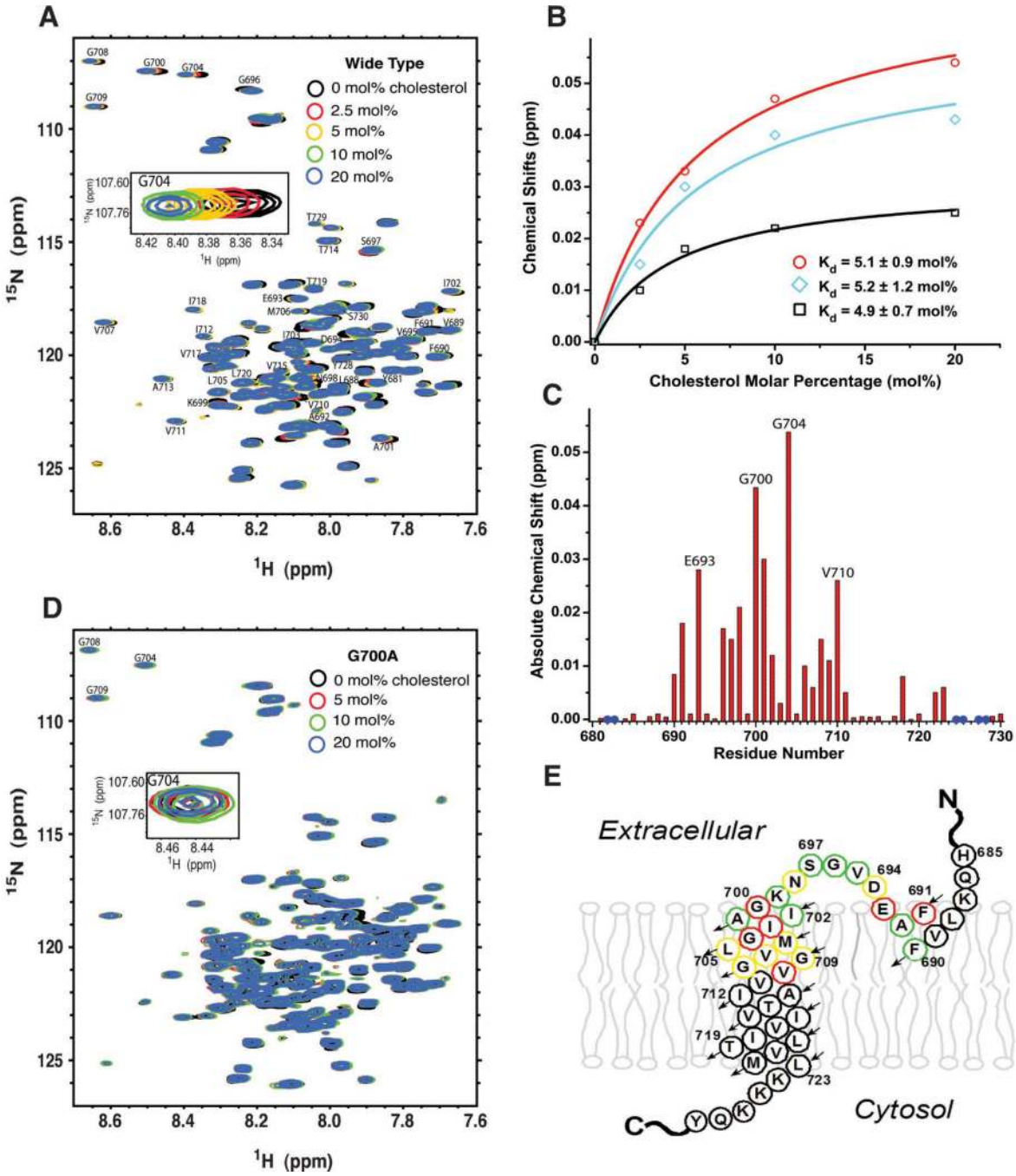

Fig. 3.

Cholesterol binding to C99 in bicelles. (**A**) Cholesterol titration of U-^{15}N-C99 in dihexanoylphosphatidylcholine-dimyristoylphosphatidylcholine (DHPC-DMPC) bicelles, as monitored by ^{1}H,^{15}N–transverse relaxation optimized spectroscopy NMR. Cholesterol was varied from 0 to 20 mol % (relative to total moles of lipid). ppm, parts per million. T, Thr; V, Val; I, Ile; F, Phe; M, Met; D, Asp; A, Ala; Y, Tyr. (**B**) Changes in amide ^{1}H NMR chemical shifts for E693 (black), G700 (light blue), and G704 (red) in response to cholesterol titration of WT C99. Also shown are the fits of a 1:1 binding model to each data set, with resulting K_d values for complex formation indicated as well. Units of mole percent

are appropriate to describe the binding of two molecules that are both associated with model membranes {mole percent = [moles cholesterol/(moles DMPC + moles cholesterol)] × 100}. (**C**) Changes in ^{1}H NMR chemical shifts for WT C99 in response to the addition of cholesterol to 20 mol % concentration. Results are shown for residues at or near the cholesterol binding site. (**D**) Titration of the G700A mutant form of C99 with cholesterol. (Data for other C99 mutants are shown in fig. S8). (**E**) Results of Ala-scanning mutagenesis. Residue color indicates the impact on cholesterol binding of substituting each position in the 690 to 710 range, as assessed by NMR. Red indicates that mutation to Ala for that site eliminates binding, yellow indicates significantly attenuated binding, and green indicates that mutation results in little change in cholesterol binding affinity.